Int. J. Electrochem. Sci., 10 **(2015)** 10045 - 10060

International Journal of
ELECTROCHEMICAL
SCIENCE
www.electrochemsci.org

Thermodynamic Analysis of a Hybrid System Integrating an Alkaline Fuel Cell with an Irreversible Absorption Refrigerator

Mingzhou Zhao, Hongwei Zhao, Mengmeng Wu, Houcheng Zhang[*] *, Ziyang Hu, Ziqi Zhao*

Department of Microelectronic Science and Engineering, Ningbo University, Ningbo 315211, China
[*]E-mail: zhanghoucheng@nbu.edu.cn

Received: 14 July 2015 / *Accepted:* 29 September 2015 / *Published:* 4 November 2015

A hybrid system integrating an irreversible absorption refrigerator to an AFC (alkaline fuel cell) is proposed, where the AFC electrochemically converts the chemical energy contained in the inlet hydrogen into electricity and waste heat, the electricity is delivered to the external load and the waste heat is subsequently transferred to drive the absorption refrigerator for cooling purpose. By considering the main irreversible losses in the hybrid system, the operating current density interval of the AFC allows the absorption refrigerator to exert its function is determined and the numerical expressions for the equivalent power output and efficiency of the hybrid system under different operating conditions are specified. Numerical calculations show that the maximum power density and the corresponding efficiency of the hybrid system can be respectively increased by 2.6% and 3.0% compared to that of the stand-alone AFC. The general performance characteristics and optimum criteria for the hybrid system are revealed. Comprehensive parametric analyses are conducted to reveal the effects of internal irreversibility of the absorption refrigerator, operating current density, operating temperature and operating pressure of the AFC, and the heat loss from the AFC to the environment on the performance of the hybrid system.

Keywords: Alkaline fuel cell; Absorption refrigerator; Hybrid system; Irreversible loss; Thermodynamic analysis

1. INTRODUCTION

The dual effects of the limited fossil fuel sources and environment pollution have shown the requirement of innovative energy generation systems to not only increase efficiency but also reduce harmful emissions. Fuel cells are static energy conversion devices directly convert the chemical energy of fuels into electrical energy and waste heat with water as byproduct, which have the potential to lower the environmental burden of meeting domestic energy needs, particularly greenhouse gas emissions and primary energy consumption [1, 2]. Among various kinds of fuel cells [3-6], AFCs

(alkaline fuel cells) and PEMFCs (proton exchange membrane fuel cells) are regarded as the two kinds of most promising fuel cells, due to their low working temperature and high efficiency [7]. AFCs have advantages over traditional PEMFCs due to alkaline media provides a less corrosive environment to the catalysts and electrode [8, 9]. AFCs can be also manufactured at less cost and using non-noble materials for catalysts and their balance of plant are less complicated than that of PEMFC systems [10]. Moreover, the perceived disadvantage of carbon dioxide intolerance was found to be a minor problem, as cost effective removal can be achieved with chemical-, thermal- or electrical-swing adsorbers [11, 12]. In this prospect, the research and development activities in AFC technology are rising again, leading to new market opportunities, further efficiency improvement and cost reduction.

However, the comparative low power density of AFCs has become a critical factor that restricts its widely commercialization [13, 14]. The maximum power density for AFCs has undergone many advances due to the progresses in catalysts, electrode materials, optimized operating conditions and fuel cell design [15]. Alternatively, the equivalent maximum power density for such low-temperature fuel cells can be also effectively elevated by exploiting cogeneration systems to recover the waste heat for other applications [12, 16-21]. Staffell et al. [12] assessed a life cycle of an AFC based CHP system using a literature review of cell, stack and system construction. It was concluded that the operating lifetime of the AFCs stack could be greatly improved and a competitive lifetime of 20-40 thousand hours could be expected. Hwang et al. [16, 17] developed a waste heat recovery subsystem and implemented it in a PEMFC cogeneration system to simultaneously generate electricity and hot water. Ishizawa et al. [18] presented a PAFC (phosphoric acid fuel cell) energy system for telecommunication cogeneration systems, where the PAFCs are applied to provide electrical power to telecommunication equipment and the waste heat is used by absorption refrigerators to cool the telecommunication rooms. Zhao et al. [19] carried out the parametric studies on a hybrid power system by integrating a PEMFC stack with an organic Rankine cycle to recover the waste heat from PEMFC stack. Yang et al. [20] evaluated the performance of a hybrid system composed of an AFC and a thermoelectric generator, the equivalent maximum power density for the AFC was found to be increased by up to 23%. Zhang et al. [21] established a highly unified hybrid system coupling an AFC with a three-heat-reservoir cycle which may function as either a refrigerator or a heat pump. They determined the maximum equivalent power output and efficiency of the hybrid system and found that the waste heat produced in the AFC can be readily used in such a hybrid system.

Absorption refrigerator enables to produce cold through thermodynamic processes without providing any electrical work, which has a great potential for reducing of the negative impacts on the environment [22, 23]. Besides being environmentally friendly, absorption refrigerator also has many other advantages such as being highly reliable, having absolute low noise, adapting to various heat sources with moderate temperature (e.g. waste heat from various industries, solar energy and geothermal energy) [24-26]. The ability to use unwanted heat causes such system to gain popular in the commercial cooling for energy recycle applications. Obviously, the waste heat generated in the AFC can be further transferred to drive the absorption refrigerator for cooling purpose, and thus, the equivalent maximum power density of the AFC can be effectively enhanced.

In this work, a hybrid system integrating an AFC with an absorption refrigerator to simultaneously produce electricity and cooling is proposed to improve the overall power output and

thus efficiency. The analytical expressions for power output and efficiency of the hybrid system are derived by considering the multi-irreversibilities such as the external and internal irreversibilities of the absorption refrigerator, electrochemical irreversible losses inside the AFC, and heat leakage from the AFC to the surroundings. The general performance characteristics and optimum criteria of the hybrid system will be revealed and the operating current density region of the AFC enables the absorption refrigerator to exert its function will be determined. The effects of some operating conditions and designing parameters on the performance of the hybrid system will be discussed by comprehensive parametric analyses.

2. An AFC/ABSORPTION REFRIGERATOR HYBRID SYSTEM

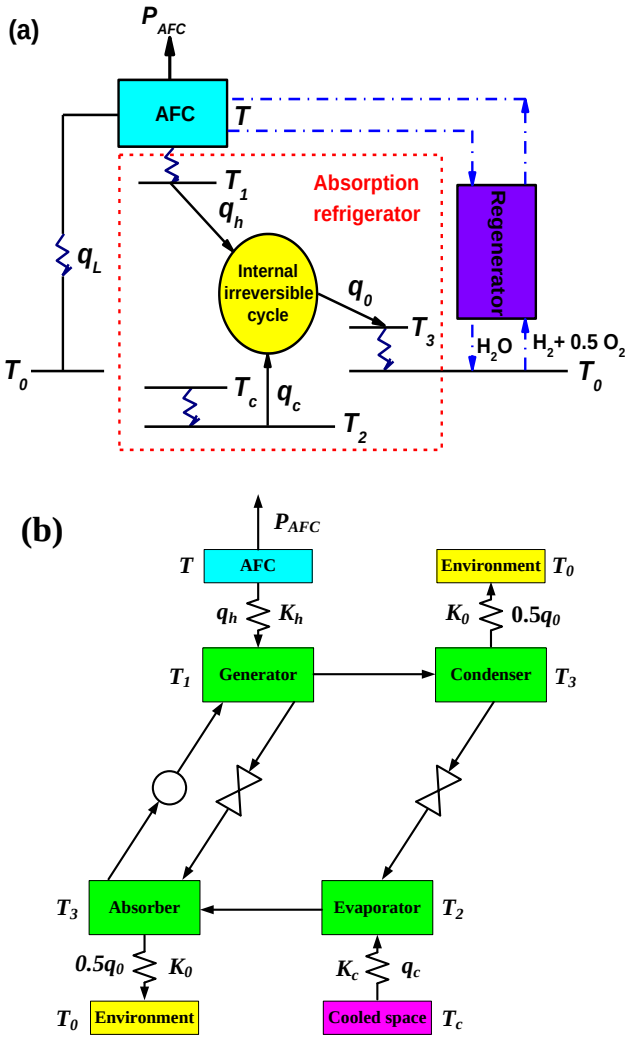

Figure 1. Schematic diagrams of (a) an AFC/absorption refrigerator hybrid system and (b) an absorption refrigerator.

The AFC/ absorption refrigerator hybrid system mainly consists of an AFC, an absorption refrigerator and an auxiliary regenerator, as schematically shown in Fig. 1, where P_{AFC} is the electric

power output of the AFC, q_h is the heat-transfer rate from the AFC at temperature T to the generator, q_c is the heat-transfer rate from the cooled space at temperature T_c to the evaporator, q_0 is the total heat-transfer rate from the condenser and absorber to the environment at temperature T_0, and q_L is the heat-leakage rate from the AFC to the environment via convective and/or conductive heat transfer. For such a hybrid system, the waste heat released in the AFC can be readily utilized in the absorption refrigerator for cooling purposes without any electric power input, and consequently, the performance of the hybrid system is expected to be better than that of the stand-alone AFC. In order to conveniently describe the mainly irreversible losses existing in the hybrid system, some simplifications and assumptions are made here [20, 27-30]: (1) Both the AFC and the absorption refrigerator are operated under steady state conditions; (2) Operating temperature and operating pressure are uniform and constants in the AFC; (3) Amounts of hydrogen and air are theoretically provided based on the electric current produced; (4) Flow of reactants is steady, incompressible and laminar; (5) Internal current density referred to the electrons transported through the electrolyte and to the fuel crossover is neglected; (6) Working fluid in the absorption refrigerator flows constantly and exchanges heat continuously with the three external heat sources; (7) Work input required by the solution pump in the absorption refrigerator is negligible; (8) Heat transfers within the system obey Newton's law.

2.1. The AFC

As demonstrated in References [20, 27], some irreversible losses are inevitably when the electrochemical reactions are occurred in an AFC, and they can be characterized in terms of activation overpotential (V_{act}), concentration overpotential (V_{con}) and ohmic overpotential (V_{ohm}). Taking these three overpotentials into account, the power output and efficiency of the AFC can be respectively expressed as [20, 27]

$$P_{AFC} = jA(E - V_{act} - V_{ohm} - V_{con}), \tag{1}$$

and

$$\eta_{AFC} = \frac{P_{AFC}}{-\Delta \dot{H}} = \frac{n_e F}{-\Delta h}\left(E - V_{act} - V_{con} - V_{ohm}\right), \tag{2}$$

where $E = \left[-\Delta g^0 + (T - T_0)\Delta s^0 + RT\ln(p_{H_2}\sqrt{p_{O_2}} / p_{H_2O})\right] \Big/ n_e F$ is the equilibrium potential; Δg^0 is the molar Gibbs free energy change at ambient temperature and atmospheric pressure, Δs^0 is the standard molar entropy change; T is the operating temperature of the AFC; R is the universal gas constant; n_e is the number of electrons transferred per hydrogen molecule; F is the Faraday's constant; $p_{\mathrm{H_2}}$, $p_{\mathrm{O_2}}$ and $p_{\mathrm{H_2O}}$ are respectively the partial pressures of $\mathrm{H_2}$, $\mathrm{O_2}$ and $\mathrm{H_2O}$, and the water produced is assumed to be in liquid phase, such that $p_{\mathrm{H_2O}} = 1$ atm; j is the current density; A is the effective polar plate area of the AFC; $V_{act} = RT\ln(j / j_0)/(\beta n_e F)$, β is the transfer coefficient, $j_0 = c_1 \exp(-c_2 / T)$ is the exchange current density, c_1 and c_2 are two constants; $V_{con} = RT\ln[j_L / (j_L - j)] / (\beta n_e F)$, j_L is the limiting current density; $V_{ohm} = jt_{ele} / \kappa$, t_{ele} is the thickness of electrolyte, κ is the specific

conductivity of the electrolyte [27]. $(-\Delta \dot{H}) = -jA\Delta h/(n_e F)$ is the total energy released per unit time, Δh is the molar enthalpy change at temperature T.

2.2. The absorption refrigerator

The absorption refrigerator in the hybrid system is driven by the waste heat produced in the AFC with reasonable assumptions that the working fluid in the condenser and absorber have the same temperature (T_3) and exchange heat with the heat sinks at the same temperature (T_0) [31-34]. As shown in Fig. 1 (b), the absorption refrigerator in the hybrid system is operated between three heat reservoirs with temperatures T, T_c, and T_0, and the temperatures of the cyclic working fluids in three isothermal processes are different from those of external heat reservoirs, where T_1 is the temperature of the working fluid in the generator, T_2 is the temperature of the working fluid in the evaporator, T_3 is the temperature of the working fluid in the condenser and absorber. Taking the finite-rate heat transfer and the internal irreversible effects inside the working fluid into account, one can obtain the optimum coefficient of performance and cooling rate of the internal irreversible absorption refrigerator for a given input rate of heat q_h [34, 35]

$$\varepsilon = \frac{1}{2}\left\{\left[\left(a+\frac{I_r T_0 - T_c}{Cq_h}\right)^2 - 4T_c\left(\frac{1}{(1+B)^2 T} - \frac{1-I_r T_0/T}{Cq_h}\right)\right]^{0.5} - \left[a+\frac{I_r T_0 - T_c}{Cq_h}\right]\right\}, \tag{3}$$

and

$$q_c = \frac{q_h}{2}\left\{\left[\left(a+\frac{I_r T_0 - T_c}{Cq_h}\right)^2 - 4T_c\left(\frac{1}{(1+B)^2 T} - \frac{1-I_r T_0/T}{Cq_h}\right)\right]^{0.5} - \left[a+\frac{I_r T_0 - T_c}{Cq_h}\right]\right\}, \tag{4}$$

where $a = 1 + \dfrac{T_c - I_r B^2 T_0}{(1+B)^2 T}$, I_r is the internal irreversibility factor, $B = \left(\sqrt{b_2} - 1\right)\Big/\left(1+\sqrt{I_r b_1}\right)$, $b_1 = K_h/K_0$, $b_2 = K_h/K_c$, K_h is the heat-transfer coefficient of the generator, K_c is the heat-transfer coefficient of the evaporator, and K_0 is the heat-transfer coefficient of the condenser or absorber assuming the heat-transfer coefficient of the condenser is equal to that of the absorber [30]; $C = (1+B)^2/(A_R K)$, $A_R = A_h + A_c + A_o$ is the overall heat-transfer area of the absorption refrigerator, A_h and A_c are respectively the heat-transfer areas of the generator and evaporator, A_0 is the total heat-transfer area of the condenser and absorber, and $K = K_h\Big/\left[1+\sqrt{I_r b_1}\right]^2$.

Thus, the equivalent power output and efficiency of the absorption refrigerator can be, respectively, expressed as [37, 38]

$$P_{AR} = q_c\left|1-\frac{T_0}{T_c}\right| = \frac{q_h}{2}\left|1-\frac{T_0}{T_c}\right|\left\{\left[\left(a+\frac{I_r T_0 - T_c}{Cq_h}\right)^2 - 4T_c\left(\frac{1}{(1+B)^2 T} - \frac{1-I_r T_0/T}{Cq_h}\right)\right]^{0.5} - \left[a+\frac{I_r T_0 - T_c}{Cq_h}\right]\right\}, \tag{5}$$

and

$$\eta_{AR}=\frac{P_{AR}}{q_h}=\frac{1}{2}\left|1-\frac{T_0}{T_c}\right|\left\{\left[\left(a+\frac{I_rT_0-T_c}{Cq_h}\right)^2-4T_c\left(\frac{1}{(1+B)^2T}-\frac{1-I_rT_0/T}{Cq_h}\right)\right]^{0.5}-\left[a+\frac{I_rT_0-T_c}{Cq_h}\right]\right\}. \quad (6)$$

2.3. The regenerator

The regenerator is an important auxiliary device which heats the inlet reactants by using the heat in the relative high-temperature exhaust products. For a low temperature hydrogen-oxygen fuel cell, it has been proved that the waste heat contained in the exhaust product is enough to heat the inlet reactants in the regenerator so that the export temperature of the inlet rectants is ensured to attain the working temperature of the fuel cell [39]. On the other hand, the efficiencies of some regenerators with the values of 98-99% have already been reported [40]. For this reasons, it is proper to assume that the regenerator in the hybrid system performs perfect regeneration.

2.4. Power output and efficiency of the hybrid system

As illustrated in Fig. 1 (a), the total thermal energies released in the AFC are divided into two parts. The part leaked into the environment and the part transferred to the absorption refrigerator can be, respectively, expressed as [20]

$$q_L=K_LA_L(T-T_0), \quad (7)$$

and

$$q_h=-\Delta\dot{H}-P_{AFC}-q_L=-\frac{A\Delta h}{2F}\left[(1-\eta_{AFC})\,j-\frac{2Fc_3(T-T_0)}{-\Delta h}\right], \quad (8)$$

where K_L is the heat-leak coefficient and A_L is the corresponding heat-transfer area, $c_3=K_LA_L/A$ is an integrated parameter closely related to thermodynamic losses and depends on the heat-leak coefficient and the geometry configurations of the AFC.

As shown by Eq. (8), the bottoming absorption refrigerator begins to exert its function only when the condition of $q_h>0$ is fulfilled, i.e.,

$$-\Delta\dot{H}-P_{AFC}>q_L. \quad (9)$$

Combined Eq. (8), Eq. (9) can be further minutely expressed as

$$j>j_C=\left[\frac{2F}{-\Delta h(1-\eta_{AFC})}\right]\left[c_3(T-T_0)\right], \quad (10)$$

where j_C is the critical operating current density of the AFC from which the absorption refrigerator in the hybrid system starts to absorber heat from the cooled space. Based on Eq. (9) and the condition of $P_{AR}>0$, one may further numerically determine the allowable maximum current density, j_M, from which the absorption refrigerator stops working.

When $j_C<j<j_M$, based on Eqs. (1), (2), (5), (6) and (8), the equivalent power output and efficiency of the hybrid system can be, respectively, expressed as [21, 38]

$$P = P_{AFC} + \frac{q_h}{2}\left|1-\frac{T_0}{T_c}\right|\left\{\left[\left(a+\frac{I_r T_0 - T_c}{Cq_h}\right)^2 - 4T_c\left(\frac{1}{(1+B)^2 T} - \frac{1-I_r T_0/T}{Cq_h}\right)\right]^{0.5} - \left[a+\frac{I_r T_0 - T_c}{Cq_h}\right]\right\}, \quad (11)$$

and

$$\eta = \eta_{AFC} + \frac{\left|1-\frac{T_0}{T_c}\right|}{2}\left[1-\eta_{AFC}+\frac{2Fc_3(T-T_0)}{j\Delta h}\right]\left\{\left[\left(a+\frac{I_r T_0 - T_c}{Cq_h}\right)^2 - 4T_c\left(\frac{1}{(1+B)^2 T} - \frac{1-I_r T_0/T}{Cq_h}\right)\right]^{0.5} - \left[a+\frac{I_r T_0 - T_c}{Cq_h}\right]\right\}. \quad (12)$$

When $j \le j_C$ or $j \ge j_M$, the power output and efficiency of the hybrid system equal to that of the sole AFC, i.e.,

$$P = P_{AFC}, \quad (13)$$

and

$$\eta = \eta_{AFC}. \quad (14)$$

3. GENERAL PERFORMANCE CHARACTERISTICS AND OPTIMUM CRITERIA

Table 1. Parameters used in the modeling [20, 27, 28, 35, 36].

Parameter	Value
Operating pressure, P (atm)	1.0
Ideal gas constant, R (J mol^{-1} K^{-1})	8.314
Faraday constant, F (C mol^{-1})	96,485
Number of electrons, n_e	2.0
Temperature of the environment, T_0 (K)	313
Operating temperature of AFC, T (K)	353
Anode gas composition	60%H_2/40%H_2O
Cathode gas compositions	21%O_2/79%N_2
Charge transfer coefficient, β	0.1668
Limiting current density, j_L (A m^{-2})	2.0×10^3
Thickness of the electrolyte, t_{ele} (m)	1.0×10^{-3}
Polar plate area of an AFC, A (m^2)	9.0×10^{-3}
Constant, c_1 (A m^{-2})	174,512
Constant, c_2 (K)	5485
Temperature of the cooled space, T_c (K)	293
Internal irreversibility of the absorption refrigerator , I_r	1.05
Constant c_3 (W m^{-2} K^{-1})	0.9
Constant b_1	4.0
Constant b_2	0.5
Integrated parameter C (K W^{-1})	1.0

Based on Eqs. (1)-(14) and the typical parametric values summarized in Table 1 [20, 27, 28, 35, 36], the general performance characteristics of the hybrid system can be revealed through numerical calculations.

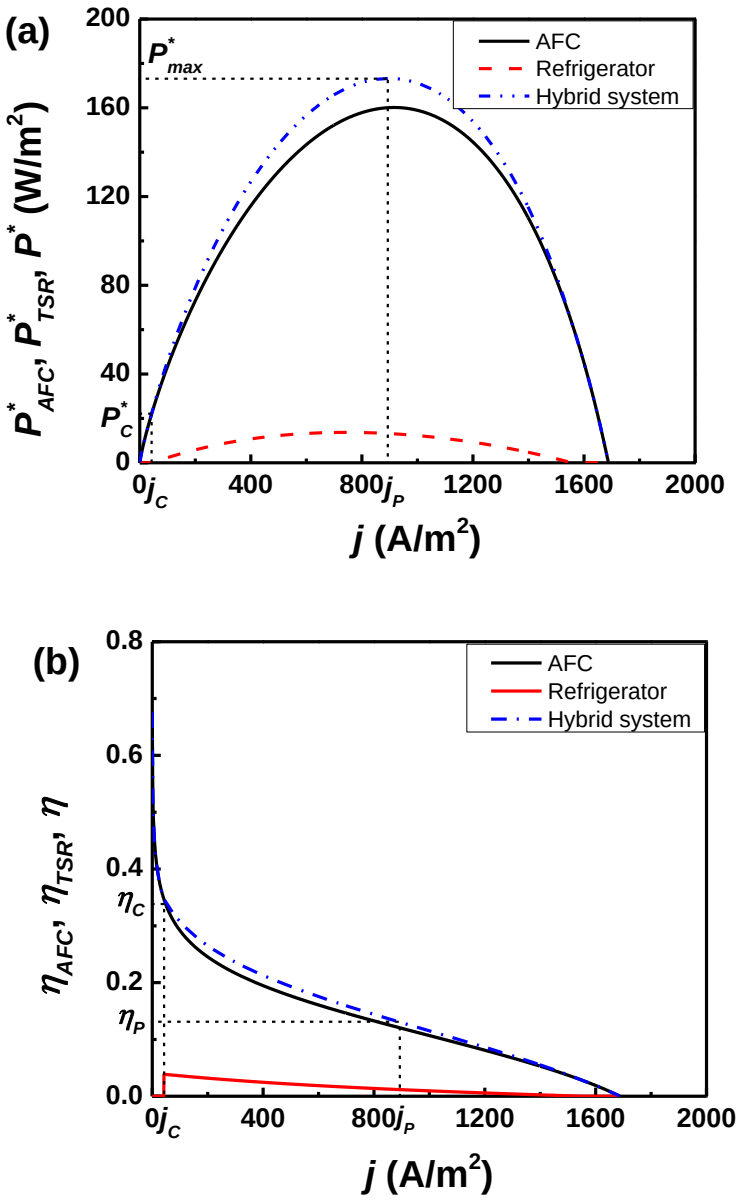

Figure 2. Curves of (a) power densities and (b) efficiencies of the AFC, absorption refrigerator, and hybrid system varying with the operating current density of the AFC, where $P^*_{PEMFC} = P_{PEMFC} / A$ and $P^*_{AR} = P_{AR} / A$ are the power densities of the AFC and absorption refrigerator, $P^* = P / A$ is the power density of the hybrid system, j_P is the operating current density corresponding to the maximum power density of the hybrid system $P^*_{\max}$, j_C and j_M are respectively the lower bound and upper bound current densities that the absorption refrigerator exerts its function, P^*_C and η_C are the power density and efficiency at the critical operating current density j_C.

Fig. 2 clearly shows the equivalent power densities and efficiencies of the AFC, absorption refrigerator and hybrid system varying with the operating current density of AFC, where $P^*_{AFC} = P_{AFC} / A$, $P^*_{AR} = P_{AR} / A$ and $P^* = P / A$ are respectively the power densities of the AFC,

absorption refrigerator, and hybrid system, $P^*_{\max}$ is the maximum value of P^*, η_P and j_P are respectively the efficiency and operating current density corresponding to $P^*_{\max}$, P^*_C and η_C are respectively the power density and efficiency of the hybrid system at the critical operating current density j_C. It is observed that the power density of the hybrid system first increases and then decreases as the operating current density is increased, while the efficiency continuously decreases with the operating current density. Fig. 2 also shows that the state of the hybrid system at the maximum power density is different from that of the AFC or absorption refrigerator at their maximum power densities, the hybrid system reaches its maximum power density at about 890 A m^{-2}, and the AFC and the absorption refrigerator reach their maximum power densities at about 920 A m^{-2} and 740 A m^{-2}, respectively. When the operating current density is situated in the region of $0 < j \le j_C$ or $j \ge j_M$, the curves of the power density and efficiency of the hybrid system are overlapped with that of the sole AFC. When the operating current density is operated in the region of $j_C < j < j_M$, the power density and efficiency of the hybrid system are larger than either that of the AFC or that of the absorption refrigerator. It clearly confirms that the performance of the AFC can be effectively enhanced by coupling an absorption refrigerator for further transferring the waste heat for cooling purpose in some specific operating regions. For the typical parameters given in Table 1, the maximum equivalent power density of the hybrid system is about 8.2% larger than that of the sole AFC, and the efficiency of the hybrid system at its maximum power density is about 6.1% larger than that of the sole AFC at its maximum power density.

As indicated by Fig. 2, when the operating current density is larger than j_P, the continuously increase in the operating current density not only lowers the efficiency but also lowers the power density. Combined both the efficiency and the power density into consideration, the hybrid system is not suggested to be operated in the region of $j > j_P$. Thus, the optimum operation region of the operating current density is located in

$$j_C < j \le j_P . \tag{15}$$

When the current density is operated in the optimum region of $j_C < j \le j_P$, the optimum regions for the power density and efficiency of the hybrid system are, respectively, given by

$$P^*_C < P^* \le P^*_{\max}, \tag{16}$$

and

$$\eta_C > \eta \ge \eta_P, \tag{17}$$

where the values of j_C, j_P, P^*_C, η_C, $P^*_{\max}$ and η_P depend on a set of designing parameters and operating conditions.

4. RESULTS AND DISCUSSION

As shown by Eqs. (11) - (14), the performance of the AFC/absorption refrigerator hybrid system not only depends on a set of designing parameters and operating conditions such as the heat-transfer area, heat-transfer coefficient and internal irreversibility factor of the absorption refrigerator, and the polar plate area, electrolyte thickness, operating current density, operating temperature and operating pressure of the AFC, but also depends on the parameter related to the heat-transfer

characteristics between the AFC and the environment, i.e., c_3. In the following, comprehensive parametric studies are implemented based on the mathematical model formulated in Section 2 and the parameters given in Table 1, and these parameters are taken as default values unless specifically mentioned.

4.1. Effects of integrated parameter C

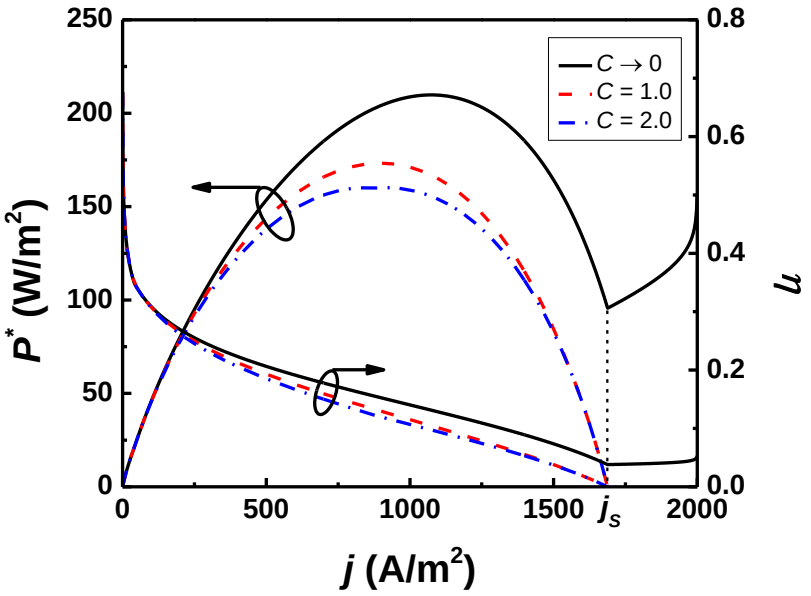

Figure 3. Effect of internal irreversibility factor on the performance of the hybrid system.

C is an integrated parameter related to the heat transfer irreversibility, internal irreversible effect and heat-transfer area of the absorption refrigerator, which dramatically affects the performance enhancement devoted from the absorption refrigerator, as shown in Fig. 3. When the current density is located in the region of $j_C < j < j_M$, the power density and efficiency of hybrid system are monotonically decreasing functions of C, and the operating current density corresponding to the maximum power density increases as C is reduced.

Detailed numerical calculation results summarized in Table 2 show that the value of j_C keeps at constant for different value of C, the values of j_M and Δj increase as C decreases. It is interesting to note from Fig. 3 that the power density and efficiency of the hybrid system can be still larger than zero even when the operating current density is larger than the stagnation current density j_S at which the AFC does not contribute electrical power any more. In this situation, the AFC in the hybrid system is operated as a heat reservoir of the bottoming absorption refrigerator rather than an electrochemical converter. When the operating current density is operated in the region of $j > j_S$, an increase in the operating current density will lead to a larger power density and a larger efficiency, however, this region exceeds the optimum operating region of $j_C < j \le j_P$. In order to increase the equivalent power density, efficiency and effective operating current density interval, efforts may be made to diminish the integrated parameter C through decreasing the internal irreversibility factor I_r and amplifying heat-

transfer coefficients (i.e., K_h, K_0 and K_c) and heat-transfer areas (i.e., A_h, A_0 and A_c). The black solid line in Fig. 3 stands for a special case that the overall heat-transfer area of the absorption refrigerator tends to be infinite large, and the heat transfer irreversibilities between the heat sources and working fluid will be disappeared. In this case, the value of j_M will exceed that of j_S and will continuously increase with the increasing j.

Table 2. The values of j_C, j_M, Δj, $P^*_{\max}$, j_P for different values of I_r, C and c_3, where the unmentioned parameters.

I_r	C	c_3	j_C	j_M	Δj	$P^*_{\max}$	j_P
		0	0	-	-	335.02	1333
	0	1.0	42	-	-	330.49	1333
		10	340	-	-	289.70	1333
		0	0	1990	1990	198.98	920
1.0	1.0	1.0	42	1991	1949	198.92	923
		10	340	1998	1659	196.67	962
		0	0	1303	1303	174.62	850
	2.0	1.0	42	1327	1285	175.22	854
		10	340	1533	1193	179.03	891
		0	0	-	-	211.34	1074
	0	1.0	42	-	-	209.79	1074
		10	340	-	-	195.86	1074
		0	0	1533	1533	173.05	893
1.05	1.0	1.0	42	1555	1513	173.25	897
		10	340	1734	1394	173.74	925
		0	0	849	849	160.14	916
	2.0	1.0	42	877	835	160.14	916
		10	340	1114	774	165.12	873
		0	0	-	-	171.98	956
	0	1.0	42	-	-	171.60	956
		10	340	-	-	168.14	956
		0	0	631	631	160.14	916
1.1	1.0	1.0	42	659	617	160.14	916
		10	340	909	569	160.14	916
		0	0	337	337	160.14	916
	2.0	1.0	42	366	324	160.14	916
		10	340	633	293	160.14	916

4.2. Effects of internal irreversibility factor

Internal irreversibility factor is a parameter to measure the irreversible losses arisen from the mass transfer, friction, eddy and other irreversible effects inside the cyclic working fluid of the absorption refrigerator [30, 36, 41]. It is seen from Fig. 4 that the power density and efficiency of the hybrid system increase with the decreasing internal irreversibility factor, and the effect of the internal

irreversibility factor on the performance of the hybrid system become more significant in the vicinity of j_P. For small internal irreversibility factor, the power density and efficiency of the hybrid system can be also still larger than zero even when the operating current density is larger than the stagnation current density j_S, but an increase in the operating current density will lead to a smaller power density and a smaller efficiency.

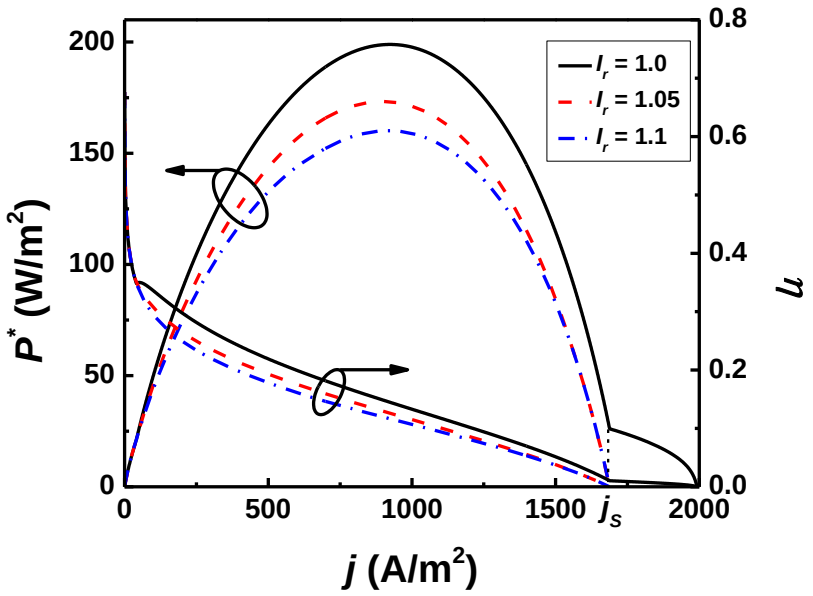

Figure 4. Effect of integrated parameter C on the performance of the hybrid system.

Table 2 indicates that the value of j_C almost keeps at constant for different values of internal irreversibility factor, while both the value of j_M and the value of effective operating current density interval Δj $(= j_M - j_C)$ increase as the internal irreversibility factor decreases. The black solid line in Fig. 4 represents a special case that the internal irreversible effect inside the absorption cycle can be neglected.

4.3. Effects of thermodynamic losses

The thermodynamic losses in the hybrid system mainly include the heat-leak from the AFC to the environment, which are respectively represented by $c_3(T - T_0)$, as described in Eq. (8). As shown in Fig. 5, the power density and efficiency of the hybrid system slightly increase as the parameter c_3 is decreased when $j < j_P$, while both of them slightly decrease as the parameter c_3 is decreased when $j > j_P$. Table 2 shows that the values of j_C and j_M shift to larger ones and the value of Δj decreases as the parameter c_3 is increased. To reduce the thermodynamic loss in the hybrid system, higher efficiency regenerators and better heat insulation materials are more favorable. The black solid line in Fig. 5 represents a special case that the heat-leak from the AFC to the environment can be negligible. In this case, the absorption refrigerator in the hybrid system starts to absorber heat from the cooled

space accompanying the operation of AFC. To reduce the thermodynamic loss in the hybrid system, better heat insulation materials for AFC are more favorable.

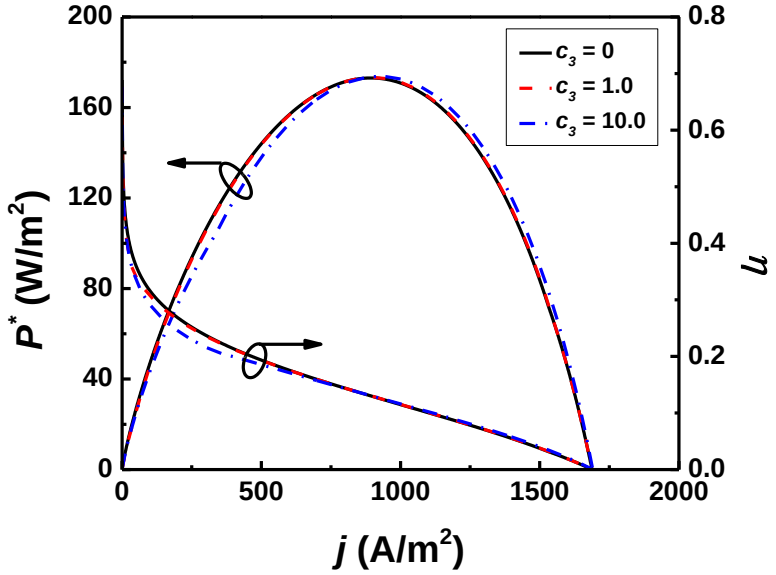

Figure 5. Effect of thermodynamic losses on the performance of the hybrid system.

4.4. Effects of operating temperature

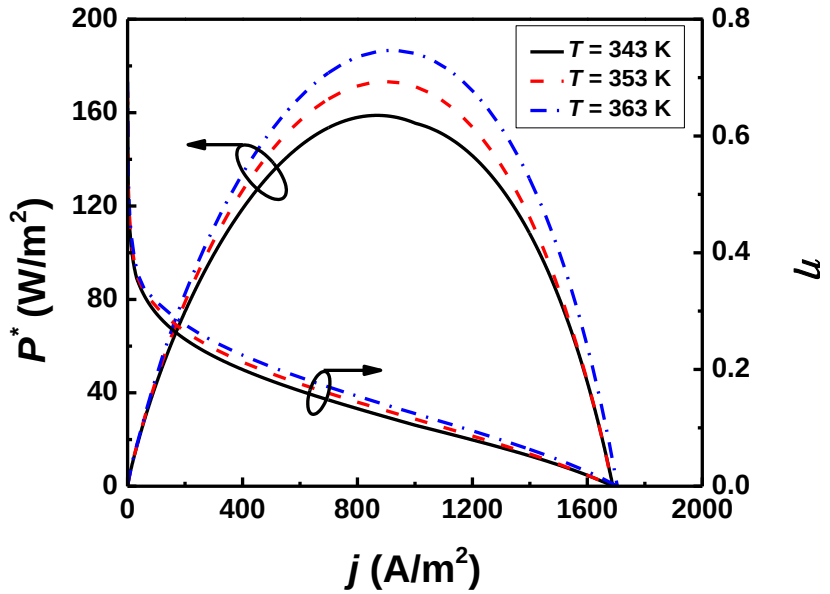

Figure 6. Effect of operating temperature on the performance of the hybrid system.

Operating temperature of the AFC is an important operating condition that not only affects the performance of the AFC but also affects the performance of the absorption refrigerator. As shown in Fig. 6, both the power density and the efficiency of the hybrid system increase as the operating

temperature increases, the operating current density corresponding to the maximum power density also increases with the increasing operating temperature, and the effect of the operating temperature on the performance of the hybrid system become more significant in the vicinity of j_P. At a higher working temperature, the ionic conductivity in the electrolyte is more efficient, leading to a smaller ohmic overpotential and larger cell voltage and thus better performance of the AFC. In addition, the larger operating temperature creates a larger temperature gap between the AFC and the working fluid of the absorption refrigerator, which is benefit to improve the performance of the absorption refrigerator. Numerical calculations show that the values of j_C, j_M and Δj shift to larger ones as the operating temperature is increased.

4.5. Effects of operating pressure

Operating pressure of AFC is another important operating condition that not only affects the performance of the AFC but also affects the amount of the waste heat and thus the performance of the absorption refrigerator.

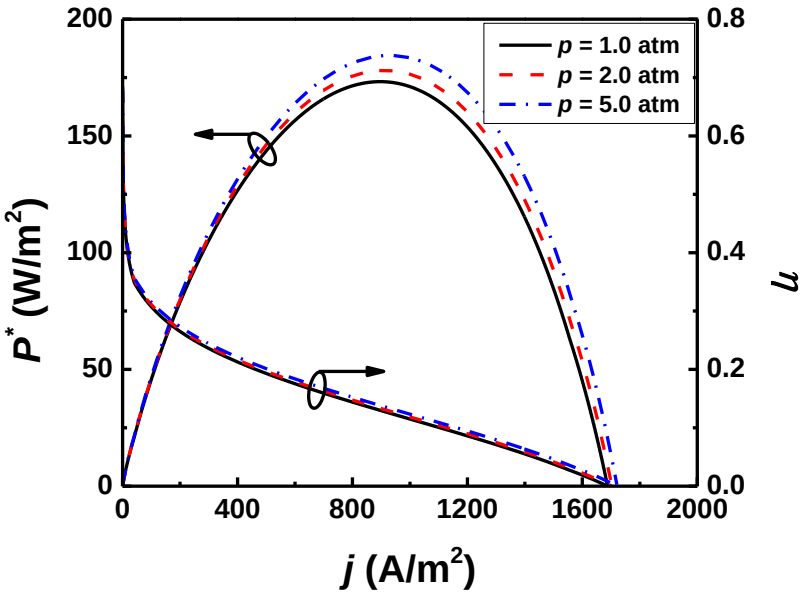

Figure 7. Effect of operating pressure on the performance of the hybrid system.

As shown in Fig. 7, both the power density and the efficiency of the hybrid system increase as the operating pressure increases, the operating current density corresponding to the maximum power density also increases with the increasing operating pressure. The effect of the operating pressure on the performance of the hybrid system mainly happens in the vicinity of j_P. Numerical calculations show that the values of j_C, j_M and Δj shift to larger ones with the increasing operating temperature. Generally, higher operating pressure is more favorable for the performance improvement, but higher operating pressure will also cost more electrical energy to compress the inlet fuel and oxidant, and thus

1 atm is always chosen as the operating pressure. The black solid line in Fig. 7 represents a special case that the operating pressure is 1 atm.

5. CONCLUSIONS

An AFC-based absorption refrigerator hybrid system consists of an AFC, an absorption refrigerator and a regenerator is proposed to harvest the waste heat generated in the AFC. By considering the main electrochemical and thermodynamic irreversible effects existing in the system, the operating current density interval of the AFC enables the absorption refrigerator to exert its function is determined and the analytical expressions for evaluating the performance of the hybrid system are specified under different operating condition. It is found that the performance can be effectively improved by coupling an absorption refrigerator to the AFC for cooling purpose. The general performance characteristics and optimum criteria of the hybrid system are revealed. The effects of internal irreversibility of the absorption refrigerator, operating current density, operating temperature, operating pressure of the AFC, and thermodynamic losses on the performance of the hybrid system are discussed through numerical calculations.

ACKNOWLEDGMENTS
This work has been supported by the Natural Science Foundation of Zhejiang Province of China (Grant Nos. LQ14E06002, LQ14F04002), the National Natural Science Foundation of China (Grant No. 51406091), the Zhejiang Open Foundation of the Most Important Subjects (Grant No. xkzw108), the Scientific Research Project of Ningbo University (Grant No. XYL14005), and the K. C. Wong Magna Fund in Ningbo University.

References

1. G. J. K Acres, *J. Power Sources*, 100(2001)60.
2. A. Kirubakaran, S. Jain and R. K. Nema, Renew. *Sust. Energy Rev.*, 13(2009)2430.
3. Y. Wang, K. S. Chen, J. Mishler, S. C. Cho and X. C. Adroher, *Appl. Energy*, 88(2011)981.
4. O. Z. Sharaf and M. F. Orhan, *Renew. Sust. Energy Rev.*, 32(2014)810.
5. N. Sammes, R. Bove and K. Stahl, *Curr. Opin. Solid St. M.*, 8(2004)372.
6. H. B. Hassan, M. A. Abdel Rahim, M. W. Khalil and R. F. Mohammed, *Int. J. Electrochem. Sci.*, 9(2014)760.
7. X. Song and D. Zhang, *Energy*, 70(2014) 223.
8. F. Bidaulta, D. J. L. Brettb, P. H. Middletonc and N. P. Brandon, *J. Power Sources*, 187(2009)39.
9. J. R. Varcoe and R. C. T. Slade, *Fuel Cells*, 5(2005)187.
10. X. Song and D. Zhang, *Energy*, 70(2014)223.
11. E. Gülzow and M. Schulze, *J. Power Sources*, 127(2004)243.
12. I. Staffell and A. Ingram, *Int. J. Hydrogen Energy*, 35(2010)2491.
13. M. C. Kimble and R. E. White. *J. Electrochem. Soc.*, 138(1991)3370.
14. W. Gao, *IEEE T. Veh. Technol.*, 54(2005)46.
15. I. Verhaert, S. Verhelst, G. Janssen, G. Mulder and M. De Paepe, *Int. J. Hydrogen Energy*, 36(2011)11011.

16. J. J. Hwang, M. L. Zou, W. R. Chang, A. Su, F. B. Weng and W. Wu, *Int. J. Hydrogen Energy*, 35(2010)8644.
17. J. J. Hwang and M. L. Zou. *J. Power Sources*, 195(2010)2579.
18. M. Ishizawa, S. Okada and T. Yamashita, *J. Power Sources*, 86(2000)294.
19. P. Zhao, J. Wang, L. Gao and Y. Dai, *Int. J. Hydrogen Energy*, 37(2012)3382.
20. P. Yang, Y. Zhu, P. Zhang, H. Zhang, Z. Hu and J. Zhang, *Int. J. Hydrogen Energy*, 39(2014)11756.
21. X. Zhang and J. Chen, *J. Power Sources*, 196(2011)10088.
22. M. O. Abdullah and T. C. Hieng, *Appl. Energy*, 87(2010)1535.
23. P. A. N. Wouagfack and R. Tchinda, *Renew. Sus. Energy Rev.*, 21(2013)524.
24. O. Bautista and F. Mendez, *Energy Convers. Manag.*, 46(2005)433.
25. R. Fathi, C. Guemimi and S. Ouaskit, *Renew. Energy*, 29(2004)1349.
26. M. P. Islam and T. Morimoto, *Renew. Energy*, 72(2014)367.
27. H. Zhang, G. Lin and J. Chen, *Energy*, 36(2011)4327.
28. I. Verhaert, M. De Paepe and G. Mulder, *J. Power Sources*, 193(2009)233.
29. P. Yang and H.Zhang, *Energy*, 85(2015)458.
30. P. A. Ngouateu Wouagfack and T. Tchinda, *Int. J. Refrigeration*, 40(2014)404.
31. A. Kodal, B. Sahin, I. Ekmekci and T. Yilmaz, *Energy Convers. Manage.*, 44(2003)109.
32. J. Chen and J. A. Schouten, *Energy Convers. Manage.*, 39(1998)999.
33. P. A. Ngouateu Wouagfack and R. Tchinda, *Int. J. Refrigeration*, 34(2011)1008.
34. B. A. M. Nouadje, Ngouateu, P. A. Wouagfack and R. Tchinda, *Int. J. Refrigeration*, 38(2014)118.
35. G. Lin and Z. Yan, *J. Phys. D: Appl. Phys.*, 30(1997)2006.
36. G. Lin and Z. Yan, *J. Phys. D: Appl. Phys.*, 32(1999)94.
37. X. Zhang and J. Chen, *J. Power Sources*, 196(2011)10088.
38. X. Chen, Y. Wang and Y. Zhou, *Int. J. Electrical Power Energy Sys.*, 63(2014)429.
39. X. Zhang, X. Chen, B. Lin and J. Chen, *Int. J. Hydrogen Energy*, 36(2011)2190.
40. S. Bhattacharyya and D. A. Blank, *Int. J. Energy Res.*, 24(2000)539.
41. L. Chen, S. Gao and H. Zhang, *Int. J. Electrochem. Sci.*, 8(2013)10772.